Goethe-Universität Frankfurt am Main
Institute for theoretical physics
March 2018

Mass implementation to lattice cut-off effects in QCD thermodynamics with chemical potential

Bachelor Thesis

Florian Eisenhut

First supervisor: Prof. Dr. Owe Philipsen
Second supervisor: Junior Prof. Dr. Marc Wagner

Table of Content

1 Introduction

From today's perspective, objective matter can be explained through the so called *standard model*. It contains the group of quarks with six flavors (up, down, strange, charm, bottom and top), the six leptons (electron, muon and tau, as well as their neutrino partners), the gauge bosons (gluon, photon, Z boson and $W^{\pm}$ bosons) and the scalar Higgs boson. Additionally, it also describes three, out of four, fundamental forces: the electromagnetic, weak and strong interaction.[1]

The strong interaction between quarks and gluons is described by a field theory called *Quantum Chromodynamics* (QCD). The theory therefore introduces the charge of three different colors. However, the color is not only carried by the quarks, but also by the gluons themselves. In nature, only colorless objects like mesons, quark and anti quark which carry color and anti-color, or baryons, three quarks which carry all three colors, can be observed (confinement)[2]. An exception is the Quark-Gluon-Plasma which can occur under extreme conditions such as high temperature or density. In this state the quarks and gluons are expected to be quasi-free [3].

This thesis only concentrates on thermodynamic systems with the class of fermions, particles with half-integer spin. Each fermion has a corresponding antiparticle. Since the class of baryons, mentioned above, are particles with half-integer spin, they belong to the group of fermions.

In order to describe a system of particles, in a given volume which is in contact with a heat bath, the theory of statistical mechanics is used. These systems can be described through a choice of ensembles like the canonical or the grand canonical ensembles. While the canonical ensemble is a system where the volume and the particle number is fixed and the system can exchange energy with the heat bath, the

grand canonical ensemble also allows the exchange of particles with the heat bath. In the thermodynamic limit, where the volume goes to infinity, both ensembles will lead to the same description [4]. In this thesis, the grand canonical ensemble is chosen through the most direct description of quantum field theory.

Within this thesis, the cut-off effects of thermodynamic quantities, like pressure and fermion density, are considered for massive Wilson fermions. Therefore, the paper [5] serves as a reference, in which cut-off effects of massless fermions are considered. By implementing the mass into the relevant equations, doing similar expansions and some further steps, comparable results can be achieved. By a subsequent graphical representation, the numerically calculated results for the pressure and density, in the massless and massive case can be compared.

2 Theory

This chapter introduces the main theories in order to understand this thesis; therefore an overview of QCD in the contiuum, as well as QCD on the lattice (LQCD) is portrayed. Additionally the last section of this chapter discusses the different relations to statistical mechanics.

2.1 QCD in the continuum

With Quantum Chromodynamics (QCD), a fundamental field theory, it is possible to describe the behavior and interactions of color-charged particles like quarks and gluons. Therefore the action $S\left[\psi, \overline{\psi}, A\right]$ of the theory, is introduced. By performing a Wick rotation which means to switch to imaginary time $t = \mathrm{i}\tau$, the action can be expressed in the Euclidean space instead of the Minkowski space. Also, the action can be separated into a fermionic and a gluonic part [6, pp. 26–31] and thus reads

$$S[\psi, \overline{\psi}, A] = S_F[\psi, \overline{\psi}, A] + S_G[A] \tag{2.1}$$

$$S_F[\psi, \overline{\psi}, A] = \sum_{f=1}^{N_f} \int \mathrm{d}^4x \; \overline{\psi}^{(f)}(x) \left(\gamma_\mu(\partial_\mu + iA_\mu(x)) + m^{(f)}\right) \psi^{(f)}(x) \tag{2.2}$$

$$S_G[A] = \frac{1}{2g^2} \int \mathrm{d}^4x \; tr[F_{\mu\nu}(x)F_{\mu\nu}(x)], \tag{2.3}$$

where the fermion fields are described by the Dirac 4-Spinors $\psi^{(f)}(x)$, $\overline{\psi}^{(f)}(x)$ and the gluons by the gauge fields $A_\mu(x)$ with the space-time position x. $m^{(f)}$ defines the mass of the quarks with the flavor index f that runs from 1 to N_f. γ_μ stands for the Euclidean Dirac-Matrices and g for the coupling strength of the gauge fields to the quarks. $F_{\mu\nu}(x)$ denotes the field strength tensor and is defined as

$$F_{\mu\nu}(x) = \partial_\mu A_\nu(x) - \partial_\nu A_\mu(x) + i[A_\mu, A_\nu]. \tag{2.4}$$

Since the equations are in Euclidean space, only lower indices are used. By separating the action, the fermionic part describes the quark fields and the interaction with gluons, while the gluonic part describes only the propagation and interaction of the gluons.

With the path integral formalism, a correlator in the continuum [6, p. 18] can be expressed as

$$\left\langle \hat{O}_2(\tau)\hat{O}_1(0) \right\rangle = \frac{1}{Z} \int \mathcal{D}[\psi, \overline{\psi}]\mathcal{D}[A] e^{-S[\psi,\overline{\psi},A]} O_2[\psi(\tau), \overline{\psi}(\tau), A(\tau)] O_1[\psi(0), \overline{\psi}(0), A(0)], \tag{2.5}$$

$$Z = \int \mathcal{D}[\psi, \overline{\psi}]\mathcal{D}[A] e^{-S[\psi,\overline{\psi},A]}, \tag{2.6}$$

$$\mathcal{D}\left[\psi, \overline{\psi}\right] := \prod_{x\in\mathbb{R}^4} \prod_{f,\alpha,c} \mathrm{d}\psi^{(f)}(x)_{\overset{\alpha}{c}} \, \mathrm{d}\overline{\psi}^{(f)}(x)_{\overset{\alpha}{c}}, \quad \mathcal{D}[A] := \prod_{x\in\mathbb{R}^4} \prod_{\mu} \mathrm{d}A_\mu(x). \tag{2.7}$$

Here, $\hat{O}_2(\tau)$ and $\hat{O}_1(0)$ are operators built from field operators, whereas $O_2[\psi(\tau), \overline{\psi}(\tau), A(\tau)]$ and $O_1[\psi(0), \overline{\psi}(0), A(0)]$ are functionals of the fields to the Euclidean time τ, respectively 0. $\mathcal{D}\left[\psi, \overline{\psi}\right]$ and $\mathcal{D}[A]$ are the measures of the integrals and Z denotes the partition function.

Generally an expression like this is not exactly solvable. That is why perturbation theory will be used to calculate the path integral. However in the case of energy scales for hadronic matter, the traditional perturbation theory fails. That is caused by the strong running coupling $\alpha_S(\Lambda_{QCD}) \approx \mathcal{O}(1)$ [3, p. 15]; therefore the lattice approach is chosen and will be introduced in the next section.

2.2 QCD on the lattice

Lattice QCD (LQCD) is a well-established approach to solve QCD in low energy regions where analytic or perturbative calculations fail [7]. It has been proven that the replacement of the space-time by an Euclidean lattice is an efficient approach for theoretical understanding, as well as for computational analysis. LQCD is based on a discretization of the continuous space-time into a four dimensional lattice.

$$\begin{aligned}\Lambda :=&\{n = \{n_1, n_2, n_3, n_4\} \mid \\ &n_i = 0, 1, \ldots, N_\sigma - 1 \ \forall \ i = 1, 2, 3 \ ; \ n_4 = 0, 1, \ldots, N_\tau - 1\}\end{aligned} \tag{2.8}$$

Here n is a vector which labels a point in space-time. All points are separated by the lattice constant a that has the physical dimension of length.

$$x \in \mathbb{R},^4 \to an, \ n \in \Lambda \tag{2.9}$$

Since the lattice has a finite size, it is convenient to choose periodic boundary conditions, i.e. $n_j = N$ is identified as $n_j = 0$. In this way, the spinors are defined on the lattice points

$$\psi(x) \to \psi(an) \equiv \psi(n). \tag{2.10}$$

The partial derivative is discretized in a symmetric form

$$\partial_\mu \psi(x) \to \frac{1}{2a} \left[\psi(n + \hat{\mu}) - \psi(n - \hat{\mu})\right], \tag{2.11}$$

where $\hat{\mu}$ is defined as the unit vector in μ-direction and the integral is replaced by a sum over Λ

$$\int d^4x \to a^4 \sum_{n \in \Lambda}. \tag{2.12}$$

2.2.1 Naive discretization of fermions

Applying the transformations (2.10), (2.11) and (2.12) to the continuum fermion action (2.2), the lattice fermion action for free fermions (set $A_\mu = 0$ in (2.2)) [6, p. 33] can be written as

$$S_F^0[\psi,\overline{\psi}] = a^4 \sum_{n\in\Lambda} \overline{\psi}(n) \left(\sum_{\mu=1}^{4} \gamma_\mu \frac{\psi(n+\hat{\mu}) - \psi(n-\hat{\mu})}{2a} + m\psi(n) \right). \tag{2.13}$$

To keep the fermion action (2.13) invariant under gauge transformations, the gauge fields $U_\mu(n)$ are introduced [6, pp. 33–34]. They are elements of the SU(3) gauge group and transform like

$$U_\mu(n) \to U'_\mu(n) = \Omega(n) U_\mu(n) \Omega(n+\hat{\mu})^\dagger, \tag{2.14}$$

where $\Omega(n) \in$ SU(3) for each lattice site n. Since these gauge fields are oriented and connecting the sites n and $n+\hat{\mu}$ they are often called *link variables*. Moreover, it is also possible to define a link variable in the opposite direction that connects n and $n-\hat{\mu}$:

$$\begin{aligned} U_{-\mu}(n) &\equiv U_\mu(n-\hat{\mu})^\dagger \\ U_{-\mu}(n) \to\ U'_{-\mu}(n) &= \Omega(n) U_{-\mu}(n) \Omega(n-\hat{\mu})^\dagger. \end{aligned} \tag{2.15}$$

Because of the now introduced link variables, the fermion action can be more generalized to the so called *naive fermion action*

$$S_F[\psi,\overline{\psi},U] = a^4 \sum_{n\in\Lambda} \overline{\psi}(n) \left(\sum_{\mu=1}^{4} \gamma_\mu \frac{U_\mu(n)\psi(n+\hat{\mu}) - U_{-\mu}(n)\psi(n-\hat{\mu})}{2a} + m\psi(n) \right). \tag{2.16}$$

Since the action is bilinear in $\overline{\psi}$ and ψ [6, pp. 110], it can be expressed as

$$S_F[\psi,\overline{\psi},U] = a^4 \sum_{n,m\in\Lambda} \overline{\psi}(n) D(n|m) \psi(m), \tag{2.17}$$

where $D(n|m)$ denotes the naive Dirac operator on the lattice

$$D(n|m) = \sum_{\mu=1}^{4} \gamma_\mu \frac{U_\mu(n)\ \delta_{n+\hat{\mu},m} - U_{-\mu}(n)\delta_{n-\hat{\mu},m}}{2a} + m\ \delta_{n,m}. \tag{2.18}$$

2.2.2 Fermion doubling

In the trivial case of the gauge fields ($U_\mu(n) = \mathbb{1}$), the Fourier transformed Dirac operator [6, p. 111] is given by

$$\begin{aligned}\tilde{D}(p|q) &= \frac{1}{|\Lambda|}\sum_{n\in\Lambda} e^{-i(p-q)\cdot na}\left(\sum_{\mu=1}^{4}\gamma_\mu\frac{e^{+iq_\mu a}-e^{-iq_\mu a}}{2a}+m\mathbb{1}\right)\\ &= \delta(p-q)\tilde{D}(p),\end{aligned} \tag{2.19}$$

with $|\Lambda|$ being the number of all lattice points and

$$\tilde{D}(p) = m\ \mathbb{1} + \frac{i}{a}\sum_{\mu=1}^{4}\gamma_\mu \sin(p_\mu a). \tag{2.20}$$

The quark propagator can be formulated by calculating the inverse of the 4×4 matrix (2.20)

$$\begin{aligned}\tilde{D}(p)^{-1} &= \frac{1}{m\ \mathbb{1} + \frac{i}{a}\sum_\mu \gamma_\mu \sin(p_\mu a)}\\ &= \frac{1}{m\ \mathbb{1} + \frac{i}{a}\sum_\mu \gamma_\mu \sin(p_\mu a)}\times\frac{m\ \mathbb{1} - \frac{i}{a}\sum_\mu \gamma_\mu \sin(p_\mu a)}{m\ \mathbb{1} - \frac{i}{a}\sum_\mu \gamma_\mu \sin(p_\mu a)}\\ &= \frac{m\ \mathbb{1} - \frac{i}{a}\sum_\mu \gamma_\mu \sin(p_\mu a)}{m^2 + \frac{1}{a^2}\sum_\mu \sin(p_\mu a)^2}.\end{aligned} \tag{2.21}$$

Whilst looking for the poles of the quark propagator in the case of massless fermions ($m = 0$), it becomes obvious that the quark propagator on the lattice has additional poles, when compared to the quark propagator in the continuum ($a \to 0$) [6, p. 112].

$$\tilde{D}(p)^{-1}\big|_{m=0} = \frac{-ia^{-1}\sum_\mu \gamma_\mu \sin(p_\mu a)}{a^{-2}\sum_\mu \sin(p_\mu a)^2} \xrightarrow{a\to 0} \frac{-i\sum_\mu \gamma_\mu p_\mu}{p^2} \tag{2.22}$$

The continuum momentum propagator, right hand side of equation (2.22), has only one single pole at:

$$p = (0,0,0,0). \tag{2.23}$$

Since $p_\mu \in (-\pi/a, \pi/a]$ is inside of the 1st Brillouin zone, the lattice propagator, middle term of equation (2.22), has additional poles whenever the components of p are either $p_\mu = 0$ or $p_\mu = \pi/a$. The pole at the origin corresponds to a single fermion while the other 15 poles (called *doublers*) are unphysical. To get rid of the additional poles, *Wilson fermions* will be introduced in the next chapter.

2.2.3 Wilson fermions

In order to remove the doublers, Wilson suggested to add an additional term to the Dirac operator. By adding the so called *Wilson term*, the Dirac operator in momentum space [6, pp. 112–113] reads

$$\tilde{D}(p) = m\,\mathbb{1} + \frac{i}{a}\sum_{\mu=1}^{4}\gamma_\mu \sin(p_\mu a) + \mathbb{1}\frac{1}{a}\sum_{\mu=1}^{4}(1-\cos(p_\mu a)). \tag{2.24}$$

By inserting the proper pole $p_\mu = 0$ into the Wilson term, the Wilson term vanishes whereas the doublers contribute a factor of $2/a$ for each momentum component with $p_\mu = \pi/a$. These terms behave like additional mass terms which will become infinitely heavy by taking the continuum limit $a \to 0$. In this way, they will disappear from the physical spectrum.

2.2.4 The lattice path integral

The Euclidean correlators in the lattice formalism can be expressed, in a similarly way like the one in the continuum (2.5), through the lattice path integral in the form [6, pp. 39–41]

$$\begin{aligned}\langle O_2(\tau)O_1(0)\rangle = \frac{1}{Z}\int \mathcal{D}\left[\psi,\overline{\psi}\right]\mathcal{D}\left[U\right]e^{-S_F[\psi,\overline{\psi},U]-S_G[U]} \\ O_2\left[\psi(\tau),\overline{\psi}(\tau),U\big(\tau\big)\right]O_1\left[\psi(0),\overline{\psi}(0),U\big(0\big)\right],\end{aligned} \tag{2.25}$$

where the partition function Z is denoted by

$$Z = \int \mathcal{D}\left[\psi,\overline{\psi}\right]\mathcal{D}\left[U\right]e^{-S_F[\psi,\overline{\psi},U]-S_G[U]}, \tag{2.26}$$

$$\mathcal{D}\left[\psi,\overline{\psi}\right] := \prod_{n\in\Lambda}\prod_{f,\alpha,c} \mathrm{d}\psi^{(f)}(n)^{\alpha}_{c}\,\mathrm{d}\overline{\psi}^{(f)}(n)^{\alpha}_{c}\,, \quad \mathcal{D}[U] := \prod_{n\in\Lambda}\prod_{\mu=1}^{4}\mathrm{d}U_{\mu}(n). \tag{2.27}$$

In those equations, $O_1\left[\psi(0),\overline{\psi}(0),U(0)\right]$ and $O_2\left[\psi(\tau),\overline{\psi}(\tau),U(\tau)\right]$ are functionals of the fields evaluated at the Euclidean time $\tau = an_\tau$ respectively 0. $\mathcal{D}\left[\psi,\overline{\psi}\right]$ and $\mathcal{D}[U]$ denote the path integral measures, which are products of all quark field components and all link variables.

2.3 The relation to statistical mechanics

By comparing several conditions from the lattice field theory with statistical mechanics, similarities can be found. An example of this comparison is a spin system where the classical spin variables s_n are located on a $3D$ lattice [6, pp. 22]. The probability $P[s]$, in order to find the system in a specific configuration, is given by

$$P[s] = \frac{1}{Z}e^{-\beta H[s]}, \tag{2.28}$$

where β is the inverse temperature $\beta = 1/k_B T$, with the Boltzmann constant k_B and the energy of the system $H[s]$ which is a functional of the spins. Here, the partition function Z is defined by

$$Z = \sum_{\{s\}} e^{-\beta H[s]}, \tag{2.29}$$

where the sum runs over all spin configurations {s}. Comparing the expectation value of an observable O

$$\langle O\rangle = \frac{1}{Z}\sum_{\{s\}} e^{-\beta H[s]}O[s] \tag{2.30}$$

with (2.25), the similarities become obvious. The Boltzmann factor $\exp(-\beta H)$ is replaced by the weight factor $\exp(-S)$ and the sum by an integral. In order to do calculations on the lattice, the finite temporal extend N_τ is related to the temperature T by

$$\beta = aN_\tau = 1/T. \tag{2.31}$$

Here and in the following natural units will be used to set $k_B = 1$. Through equation (2.31), the limit of $\beta \to \infty$ corresponds to $T \to 0$. Since the physical extent of time is limited to β, this can be interpreted as a system of finite spatial volume and a fixed temperature [6, p. 302]. The continuum limit for such a system could be taken by $a \to 0$, while holding aN_τ fixed.

2.3.1 Introduction of the chemical potential

In order to describe a system that is not in the vacuum, an additional term that includes the chemical potential μ is added to the partition function of the grand canonical ensemble [6, pp. 312]. Thus it is given by

$$Z(T, \mu) = \mathrm{tr}\left[e^{(-H-\mu N_f)/T}\right], \tag{2.32}$$

where N_f denotes the fermion number. By defining

$$z := e^{\mu/T} \tag{2.33}$$

as the fugacity variable, the grand canonical partition function can be rewritten as a power series in z

$$Z(T, \mu) = \sum_n \underbrace{\left(e^{\mu/T}\right)^n}_{z^n} Z_n(T), \tag{2.34}$$

where n is a fixed fermion number $n \in \mathbb{Z}$. The negative values of n correspond to antifermions.

2.3.2 Thermodynamic quantities

With the defined partition function, other thermodynamic quantities like, the pressure and the fermion number density, can be defined [6, pp. 310–312]:

$$P := T\frac{\partial \ln Z}{\partial V} \tag{2.35}$$

$$n_f := \frac{T}{V}\frac{\partial \ln Z(T,\mu)}{\partial \mu}. \tag{2.36}$$

In these definitions, V stands for the spatial volume $V = (N_\sigma a)^3$.

For the case of baryons, built out of three quarks (fermions), the baryon number density can be easily calulated by the relation

$$n_B = \frac{1}{3}n_f. \tag{2.37}$$

3 Lattice cut-off effects

In order to describe physical results through numerical calculations in LQCD, the problem of lattice discretization errors has to be considered. Therefore, the reduction of cut-off effects on rather coarse lattices plays a significant role, since thermodynamic observables such as pressure or energy density are dimension four operators and thus drop like the fourth power of the lattice spacing a. For the next discussion, only cut-off effects in the fermionic sector will be handled with bulk thermodynamic quantities that are related to the derivative of the QCD partition function with respect to the temperature T or the quark chemical potential μ. [5]

Since [5] considered fermions as massless, mass will now be reintroduced to the same relations and quantities, where the same steps achieve a similar relation of cut-off effects.

3.1 Leading steps to cut-off effects

This section particularly focuses on the main aspects in the discussion of cut-off effects with free fermions in the (naive) discretization. Therefore, the partition function on a lattice of size $N_\sigma^3 N_\tau$ at temperature T and non-vanishing chemical potential μ reads [5, p. 2]

$$Z(V,T,\mu,m) = \int \prod_x \mathrm{d}\overline{\psi}_x \mathrm{d}\psi_x \; e^{-S_F}, \tag{3.1}$$

with the discretized fermionic Euclidean action

$$S_F = \sum_x \frac{1}{2}\left(\sum_{k=1}^{3}\left(\overline{\psi}_x\gamma_k\psi_{x+\hat{k}} - \overline{\psi}_x\gamma_k\psi_{x-\hat{k}}\right) + e^{\mu a}\overline{\psi}_x\gamma_4\psi_{x+\hat{4}} - e^{-\mu a}\overline{\psi}_x\gamma_4\psi_{x-\hat{4}}\right) + ma\overline{\psi}_x\psi_x. \tag{3.2}$$

Here, the entire μ-dependence of the action is shifted to the last time slice trough the transformation $\psi_{\vec{x},x_4} \to e^{-\mu x_4}\psi_{\vec{x},x_4}$, $\overline{\psi}_{\vec{x},x_4} \to e^{\mu x_4}\overline{\psi}_{\vec{x},x_4}$ and also keeps the path integral over the Grassmann valued fermion fields invariant. An introduction, for Grassmann variables can be found in [8]. Note that the chemical potential only contributes in units of the temperature $\mu/T = \mu a N_\tau$. Switching to momentum space, the action and the denominator of the fermion propagator [5, p. 2] can be expressed as

$$S_F = \sum_{p,\nu} \overline{\psi}(p)\left(i\gamma_\nu D_\nu(p,\mu) + ma\right)\psi(p), \tag{3.3}$$

$$D(\vec{p}, p_4, \mu, m) = a^2m^2 + \sum_{k=1}^{3}\sin^2(p_k a) + \sin^2(p_4 a - i\mu a). \tag{3.4}$$

Hence the partition function can be evaluated with

$$Z(V,T,\mu,m) = \prod_p D^2(\vec{p}, p_4, \mu, m), \tag{3.5}$$

where the discrete momentum values $ap_k = 2\pi n_k/N_\sigma$, $n_k = 0, \pm1, \cdots, \pm(N_\sigma/2-1)$, $N_\sigma/2$ and $ap_4 = 2\pi(n_4+1/2)/N_\tau$, $n_4 = 0, \pm1, \cdots, \pm(N_\tau/2-1), -N_\tau/2$ are caused by the finite lattice spacing. The focus of the following discussion lies on the temporal extend, hence the limit $N_\sigma \to \infty$ can be chosen, while for the temporal extent $aT \equiv 1/N_\tau$ is valid. In the next step, the pressure of a free fermion gas can be written down as

$$
\begin{aligned}
a^4 P &= 2 \int_{-\pi}^{\pi} \frac{d^3 ap}{(2\pi)^3} \frac{1}{N_\tau} \sum_{-\pi \leq ap_4 \leq \pi} \ln D(\vec{p}, p_4, \mu, m) \\
&= 2 \int_{-\pi}^{\pi} \frac{d^3 ap}{(2\pi)^3} \frac{1}{N_\tau} \sum_n \ln \left[a^2 m^2 + \sum_{k=1}^{3} \sin^2(p_k a) + \sin^2(2\pi(n+1/2)/N_\tau - i\mu a) \right].
\end{aligned}
\tag{3.6}
$$

The Matsubara sum introduced in equation (3.6) can be expressed as a sum over residues resulting from a contour integral with poles in the complex plane, like it is done in [5, 9]. Resulting from this it is possible to formulate the relation as follows [5, p. 3] (without reducing the integration and summation to the half Brillouin zone)

$$
\begin{aligned}
&\sum_n \ln \left[a^2 m^2 + \sum_{k=1}^{3} \sin^2(p_k a) + \sin^2(2\pi(n+1/2)/N_\tau - i\mu a) \right] \\
&\quad = \ln \left(1 + z e^{-N_\tau a E(\vec{p})} \right) + \ln \left(1 + z^{-1} e^{-N_\tau a E(\vec{p})} \right) + \text{const.}.
\end{aligned}
\tag{3.7}
$$

By inserting (3.7) into the pressure (3.6) and subtracting the part with zero temperature, $(Pa^4)_0 \equiv \lim_{N_\tau \to \infty} Pa^4$, ultra-violet divergences are eliminated; dividing equation (3.6) by the temperature to the fourth power, leads to

$$
\begin{aligned}
\frac{P}{T^4} &\equiv \left[Pa^4 - (Pa^4)_0 \right] N_\tau^4 \\
&= \frac{N_\tau^3}{4\pi^3} \int_{-\pi}^{\pi} \mathrm{d}^3 ap \left[\ln(1 + z\, e^{-N_\tau a E(\vec{p})}) + \ln(1 + z^{-1} e^{-N_\tau a E(\vec{p})}) \right].
\end{aligned}
\tag{3.8}
$$

Here, z again denotes the fugacity and $E(\vec{p})$ the energy of the dispersion relation, given trough the pole of the fermion propagator. In this way, equation (3.8) is normalized like in most numerical calculations and can be used as the starting point of the systematic analysis of cut-off effects for bulk thermodynamic observables. Afterwards, substituting $y_i = p_i/T = p_i a N_\tau$ as a new integration variable in (3.8) and doing an expansion of P/T^4 around $1/N_\tau = 0$ yields to the systematic corrections proportional to $1/N_\tau$.

3.2 Expansion of the dispersions relation

Wilson fermions, which were already introduced in section 2.2.3, instead of free fermions in the naive discretization, will be used in the further discussion. Since the Wilson Dirac operator has already been discussed in (2.24), it is now possible to calculate its inverse [10] which reads

$$\tilde{D}^{-1}(p) = \frac{Ma^2 - ia\sin(p_\mu a)\gamma_\mu}{M^2a^2 + \sum_\mu \sin^2(p_\mu a)}, \tag{3.9}$$

where the numerator and the denominator are multiplied by a^2. M is defined as

$$M(p) := \underbrace{m + \frac{1}{a}\sum_{i=1}^{3}(1-\cos(p_i a)) + \frac{1}{a}}_{\Omega} - \frac{1}{a}\cos(p_4 a) \tag{3.10}$$

and Ω stands for the p_4 independent part.

In order to express the energy, one can write down the dispersion relation by evaluating the poles of the Wilson fermion propagator. As a result of that, the dispersion relation reads

$$\begin{aligned} 0 &= D(\vec{p}, E = -ip_4, \mu, m) \quad \Leftrightarrow \\ 0 &= M^2a^2 + \sum_i \sin^2(p_i a) - \sinh^2(Ea) \\ &= a^2\Omega^2 - 2a\Omega\cosh(Ea) + \sum_{i=1}^{3}\sin^2(p_i a) + 1. \\ \Rightarrow \quad \cosh(aE) &= \frac{a^2\Omega^2 + \sum_i \sin^2(p_i a) + 1}{2\Omega a} \end{aligned} \tag{3.11}$$

Rewriting this expression leads to

$$\cosh(aE) = 1 + \frac{[am + \sum_i(1-\cos(p_i a))]^2 + \sum_i \sin^2(p_i a)}{2[ma + \sum_i(1-\cos(p_i a)) + 1]}. \tag{3.12}$$

Expanding the values ap_i and aE to the order p_i^4, E^4 yields

$$1+\frac{a^2E^2}{2}+\frac{a^4E^4}{24}+\mathcal{O}(a^5)=1+\frac{[am+\sum_i(\frac{a^2p_i^2}{2}-\frac{a^4p_i^4}{24})]^2+\sum_i(a^2p_i^2-\frac{a^4p_i^4}{3})}{2[ma+\sum_i(\frac{a^2p_i^2}{2}-\frac{a^4p_i^4}{24})+1]}+\mathcal{O}(a^5). \tag{3.13}$$

By rewriting E through $E(\vec{p})=E^{(0)}(\vec{p})+aE^{(1)}(\vec{p})+a^2E^{(2)}(\vec{p})+...$ [4], dividing both sides by a^2 and selecting all terms to order $\mathcal{O}(a^2)$, the equation reads

$$\begin{aligned}
&E^{(0)^2}(\vec{p})+a\left(2E^{(0)}(\vec{p})E^{(1)}(\vec{p})+mE^{(0)^2}(\vec{p})\right)\\
&+a^2\left(E^{(1)^2}(\vec{p})+2E^{(0)}(\vec{p})E^{(2)}(\vec{p})+2mE^{(0)}(\vec{p})E^{(1)}(\vec{p})+\frac{E^{(0)^4}(\vec{p})}{12}+\frac{E^{(0)^2}(\vec{p})}{2}\vec{p}^{\,2}\right)\\
&+\mathcal{O}(a^3)\\
&=\left(m^2+\vec{p}^{\,2}\right)+a\left(2m\frac{\vec{p}^{\,2}}{2}\right)+a^2\left(\frac{\vec{p}^{\,4}}{4}-\sum_i\frac{p_i^4}{3}\right)+\mathcal{O}(a^3),
\end{aligned} \tag{3.14}$$

with $\vec{p}^{\,2}=\sum_i p_i^2$. Solving the equation for $E^{(0)}$, $E^{(1)}$ and $E^{(2)}$ leads to the correction of the dispersion relation up to the order of a^2,

$$E^{(0)^2}(\vec{p})=m^2+\vec{p}^{\,2} \quad \Leftrightarrow \quad E^{(0)}=\sqrt{m^2+\vec{p}^{\,2}} \tag{3.15}$$

$$E^{(1)}(\vec{p})=-\frac{m^3}{2E^{(0)}(\vec{p})} \tag{3.16}$$

$$E^{(2)}(\vec{p})=\frac{-3m^6+15m^4E^{(0)^2}(\vec{p})-4\sum_i p_i^4E^{(0)^2}(\vec{p})-4E^{(0)^6}(\vec{p})}{24E^{(0)^3}(\vec{p})}. \tag{3.17}$$

In the case of the continuum, the well-known energy momentum relation is achieved. Here, the first correction $E^{(1)}$ is only appearing for massive particles $m\neq 0$; therefore the energy corrections to the continuum starts at $\mathcal{O}(a)$. In the case of massless fermions, the first correction vanishes and thus only the second correction contributes to the energy with a factor of

$$E^{(2)}(\vec{p}) = -\frac{1}{6E^{(0)}(\vec{p})}\left(\sum_{i=1}^{3} p_i^4 + {E^{(0)}}^4(\vec{p})\right). \tag{3.18}$$

In both cases, massless and massive fermions, the second order correction of the energy contains a term that is proportional to $a^2 \sum_\mu p_\mu^4$. Hence, the euclidean propagator is no longer rotationally invariant.

Since pressure and other quantities depend on the ratio of E/T, the variables $y_i = p_i/T = p_i a N_\tau$, $y = p/T = \sqrt{y_1^2 + y_2^2 + y_3^2}$ and $x = E^{(0)}/T = \sqrt{{m'}^2 + y^2}$ with $m' = m/T$ can be introduced to the equations (3.15),(3.16) and (3.17). Thus one obtains

$$\frac{E}{T} = x + \frac{1}{N_\tau}\left(-\frac{{m'}^3}{2x}\right) + \frac{1}{N_\tau^2}\left(\frac{-3{m'}^6 + 15{m'}^4 x^2 - 4\sum_i y_i^4 x^2 - 4x^6}{24x^3}\right). \tag{3.19}$$

$$\begin{aligned}\frac{E}{T} &= x\,[1+\Delta] = x\,[1+\Delta_1+\Delta_2] \\ &= x\left[1 + \underbrace{\frac{1}{N_\tau}\left(-\frac{m'^3}{2x^2}\right)}_{\Delta_1} + \underbrace{\frac{1}{N_\tau^2}\left(\frac{-3{m'}^6 + 15{m'}^4 x^2 - 4\sum_i y_i^4 x^2 - 4x^6}{24x^4}\right)}_{\Delta_2}\right]\end{aligned} \tag{3.20}$$

Since equation (3.20) is written in this particular way, the energy is separated into three parts: the continuum part with no corrections, the first order corrections in $1/N_\tau$ and the second order corrections with $1/N_\tau^2$.

3.3 Cut-off dependence of the pressure

In this section, the derived energy expansion (3.20) in inverse powers of N_τ will be used to discuss the systematically cut-off dependence of the pressure. In order to do so, the argument of the logarithm in equation (3.8) can be expressed like

$$1 + Ae^{-E/T} = (1 + Ae^{-x})(1 - B(1 - e^{-x\Delta})), \tag{3.21}$$

where A and B are given as $A = z$ or z^{-1} and $B(x, A) = 1/(A^{-1}e^{x} + 1)$. By continuing to expand Δ in (3.21), the form of the logarithm in (3.8) can be expressed as

$$\log(1 + Ae^{-E/T}) = \log(1 + Ae^{-x}) - Bx\Delta - \frac{1}{2}(B^2 - B)x^2\Delta^2. \tag{3.22}$$

The first term will lead to the continuum ideal gas result of the pressure and the other two terms correspond to the corrections in powers of $1/N_\tau$ and $1/N_\tau^2$. Here, Δ^2 is reduced to powers of $1/N_\tau^2$.

$$\Delta^2 = \frac{1}{N_\tau^2}\frac{m'^{\,6}}{4x^4} + \mathcal{O}\left(\frac{1}{N_\tau^3}\right) \tag{3.23}$$

By inserting equation (3.22) into the equation of the pressure (3.8), it reads

$$\begin{aligned}\frac{P}{T^4} = \frac{2}{(2\pi)^3}\int_{-\pi N_\tau}^{\pi N_\tau} \mathrm{d}^3y \Big[&\log(1 + ze^{-x}) + \log(1 + z^{-1}e^{-x}) \\ &- x\Delta\left(B(x, z) + B(x, z^{-1})\right) \\ &-\frac{1}{2}x^2\Delta^2\left(B^2(x, z) + B^2(x, z^{-1}) - B(x, z) - B(x, z^{-1})\right)\Big].\end{aligned} \tag{3.24}$$

Since the integral, from the power series in $1/N_\tau$, has limits that depend on $1/N_\tau$, it is allowed to expand its limits from $[-\pi N_\tau, \pi N_\tau]$ to infinity [11]. The corrections of this series are proportional to $e^{-N_\tau\pi}$ and by using $N_\tau = 1/aT$ they become exponentially suppressed in the continuum limit $a \to 0$.

By changing the integration into spherical coordinates and collecting the terms in powers of $1/N_\tau$, it leads to

$$\frac{P}{T^4} = \left(\frac{P}{T^4}\right)_{SB} + \left(\frac{P}{T^4}\right)_{\frac{1}{N_\tau}} + \left(\frac{P}{T^4}\right)_{\frac{1}{N_\tau^2}}, \tag{3.25}$$

with

$$\left(\frac{P}{T^4}\right)_{SB} = \frac{1}{\pi^2}\int_0^\infty \mathrm{d}y y^2 \left[\log(1+ze^{-x}) + \log(1+z^{-1}e^{-x})\right], \tag{3.26}$$

$$\left(\frac{P}{T^4}\right)_{\frac{1}{N_\tau}} = \frac{2}{(2\pi)^3}\int_0^\infty y^2\mathrm{d}y \int_0^\pi \sin\theta \mathrm{d}\theta \int_0^{2\pi} \mathrm{d}\phi\, x\Delta_1 \left(-B(x,z) - B(x,z^{-1})\right) \tag{3.27}$$

and

$$\begin{aligned}\left(\frac{P}{T^4}\right)_{\frac{1}{N_\tau^2}} =& \frac{2}{(2\pi)^3}\int_0^\infty y^2\mathrm{d}y \int_0^\pi \sin\theta \mathrm{d}\theta \int_0^{2\pi} \mathrm{d}\phi \Big[-x\Delta_2 \left(B(x,z) + B(x,z^{-1})\right) \\ & -\frac{1}{2}x^2\Delta_1^2 \left(B^2(x,z) + B^2(x,z^{-1}) - B(x,z) - B(x,z^{-1})\right)\Big].\end{aligned} \tag{3.28}$$

Δ_2 now reads

$$\Delta_2 = \frac{1}{N_\tau^2}\left(\frac{-3m'^6 + 15m'^4x^2 - 4x^6 - 4x^2y^4\left(\sin^4\theta\left(\cos^4\phi + \sin^4\phi\right) + \cos^4\theta\right)}{24x^4}\right). \tag{3.29}$$

These equations are used to compare the continuum part and the corrections with the complete unexpanded version of the pressure. Note that here also, in the case of massless fermions, where x simplifies to $x = y$, the result of the leading order term $\left(\frac{P}{T^4}\right)_{SB}$ is known from [5], as well as from [12], as

$$\begin{aligned}\left(\frac{P}{T^4}\right)_{SB} &= \frac{1}{\pi^2}\int_0^\infty \mathrm{d}y y^2 \left[\log(1+ze^{-y}) + \log(1+z^{-1}e^{-y})\right] \\ &= \frac{7\pi^2}{180}\left[1 + \frac{30}{7}\left(\frac{\mu}{\pi T}\right)^2 + \frac{15}{7}\left(\frac{\mu}{\pi T}\right)^4 + \mathcal{O}\left(\left(\frac{\mu}{T}\right)^5\right)\right].\end{aligned} \tag{3.30}$$

Another interesting relation is the ratio between the pressure and the chemical

potential μ to its fourth power P/μ^4; therefore the equations (3.25)–(3.28) become multiplied by T^4/μ^4. If the limit $T \to 0$ is chosen, the results can be compared to [13].

3.4 Cut-off dependence of the fermion density

The definition of the fermion number density in (2.36) corresponds to the derivative of the pressure with respect to the chemical potential. Applying this to the equation (3.8), the fermion density reads

$$\frac{n_f}{T^3} = \frac{2}{(2\pi)^3 a^3 T^3} \int_{-\pi}^{\pi} \mathrm{d}^3 ap \left[\frac{1}{e^{\frac{E-\mu}{T}} + 1} - \frac{1}{e^{\frac{E+\mu}{T}} + 1} \right]. \tag{3.31}$$

In the case of the expanded equations (3.25)–(3.28), the derivative with respect to μ leads to

$$\frac{n_f}{T^3} = \left(\frac{n_f}{T^3}\right)_{SB} + \left(\frac{n_f}{T^3}\right)_{\frac{1}{N_\tau}} + \left(\frac{n_f}{T^3}\right)_{\frac{1}{N_\tau^2}}, \tag{3.32}$$

with

$$\left(\frac{n_f}{T^3}\right)_{SB} = \frac{1}{\pi^2} \int_0^{\infty} \mathrm{d}y y^2 \left[\frac{1}{e^{x-\frac{\mu}{T}} + 1} - \frac{1}{e^{x+\frac{\mu}{T}} + 1} \right], \tag{3.33}$$

$$\left(\frac{n_f}{T^3}\right)_{\frac{1}{N_\tau}} = \frac{2}{(2\pi)^3} \int_0^{\infty} y^2 \mathrm{d}y \int_0^{\pi} \sin\theta \mathrm{d}\theta \int_0^{2\pi} \mathrm{d}\phi \, x\Delta_1 \left(\frac{e^{x-\frac{\mu}{T}}}{e^{x-\frac{\mu}{T}} + 1} - \frac{e^{x+\frac{\mu}{T}}}{e^{x+\frac{\mu}{T}} + 1} \right) \tag{3.34}$$

and

$$\left(\frac{n_f}{T^3}\right)_{\frac{1}{N_\tau^2}} = \frac{2}{(2\pi)^3}\int_0^\infty y^2 \mathrm{d}y \int_0^\pi \sin\theta \mathrm{d}\theta \int_0^{2\pi} \mathrm{d}\phi \left[-x\Delta_2 \left(\frac{e^{x-\frac{\mu}{T}}}{(e^{x-\frac{\mu}{T}}+1)^2} - \frac{e^{x+\frac{\mu}{T}}}{(e^{x+\frac{\mu}{T}}+1)^2} \right) - \frac{1}{2}x^2\Delta_1^2 \left(\frac{2\, e^{x-\frac{\mu}{T}}}{(e^{x-\frac{\mu}{T}}+1)^3} - \frac{2\, e^{x+\frac{\mu}{T}}}{(e^{x+\frac{\mu}{T}}+1)^3} + \frac{e^{x+\frac{\mu}{T}}}{(e^{x+\frac{\mu}{T}}+1)^2} - \frac{e^{x-\frac{\mu}{T}}}{(e^{x-\frac{\mu}{T}}+1)^2} \right) \right]. \tag{3.35}$$

By deriving equation (3.30) with respect to the chemical potential, where massless fermions are assumed, the result of the leading order fermion density term reads

$$\frac{n_f}{T^3} = \frac{1}{3}\left[\frac{\mu}{T} + \frac{\mu^3}{\pi^2 T^3} + \mathcal{O}(\mu^5)\right]. \tag{3.36}$$

This result equals the result in [12].

The fermion number density, like equation (3.31), is proportional to

$$n_f \propto \int_p \left[e^{-\frac{E-\mu}{T}} - e^{-\frac{E+\mu}{T}} \right] \quad \text{, with} \quad E = \sqrt{m^2 + \vec{p}^{\,2}} \tag{3.37}$$

thus there are two cases that can be considered for the low temperature limit ($T \to 0$) [14]. In the first case, when $\mu < m$, (3.37) approaches 0. The particles and anti-particles are Boltzmann suppressed. In the second case, when $\mu > m$, the Fermi-Dirac distribution $n = 1/(e^{-(E-\mu)/T}+1)$ becomes a step function at $T = 0$. Hence the density has its onset at $\mu = \mu_c = m$. By understanding the chemical potential as the rate of change of the free energy with respect to the number of particles, one can conclude that for $\mu < m$ there is not enough energy to create a particle. In contrast to the case of $\mu > m$, where enough energy is available, the density is nonzero.

Since the fermion number density is calculated by the derivative of p with respect to μ, the ratio of n_f/μ^3 can be considered as a further case of interest; therefore, the equations (3.32)–(3.35) become multiplied by T^3/μ^3. The results of these cal-

culations will be further discussed in sections 4.7 and 4.8.

In order to see how the gas saturates, $n_f a^3$, with the full propagator, has to be calculated. Since the exponential function in equation (3.24) has been expanded for the cut-off effects, the equations (3.32)–(3.35) are not expected to saturate.

The baryon density can be easily calculated by equation (2.37).

4 Numerical results

In this chapter, the results of the numerical calculations of thermodynamic quantities such as the pressure P and baryon density n_B, formulated in the equations above, are demonstrated.

All numerical calculations in this work are based on modules from the Numerical Algorithms Group called NAG[1]. Through these modules like [15], the integrations, appearing in the equations above, can be numerically solved.

The figures in the following sections are ordered in a particular way: The first figure shows the relation between the full and the expanded version of the quantities and after that, the first and second order corrections are presented separately. By using this form of presentation, it becomes clear how much each correction contributes. In the case of massless fermions, the first order correction, which is equal to 0, will be presented once in section 4.1 and omitted afterwards.

Quantities that are unexpanded, like the equations (3.8) and (3.31), where the energy is expressed through equation (3.12), are represented by the green line called "full propagator". The purple line describes the result of the continuum equations (3.26) and (3.33). In order to understand the full behavior of the corrections, the dark blue line shows the first order correction described by equations (3.27) and (3.34); the red line represents the second order correction described by equation (3.28) and equation (3.35). The dashed light blue line then shows the value of the continuum result plus the first order correction, whereas the orange line shows the full expanded version of the quantities where the continuum plus the first and second order correction is summed up.

[1] https://www.nag.co.uk/ [Online; accessed 26-February-2018]

4.1 Ratio of P/T^4 for massless fermions

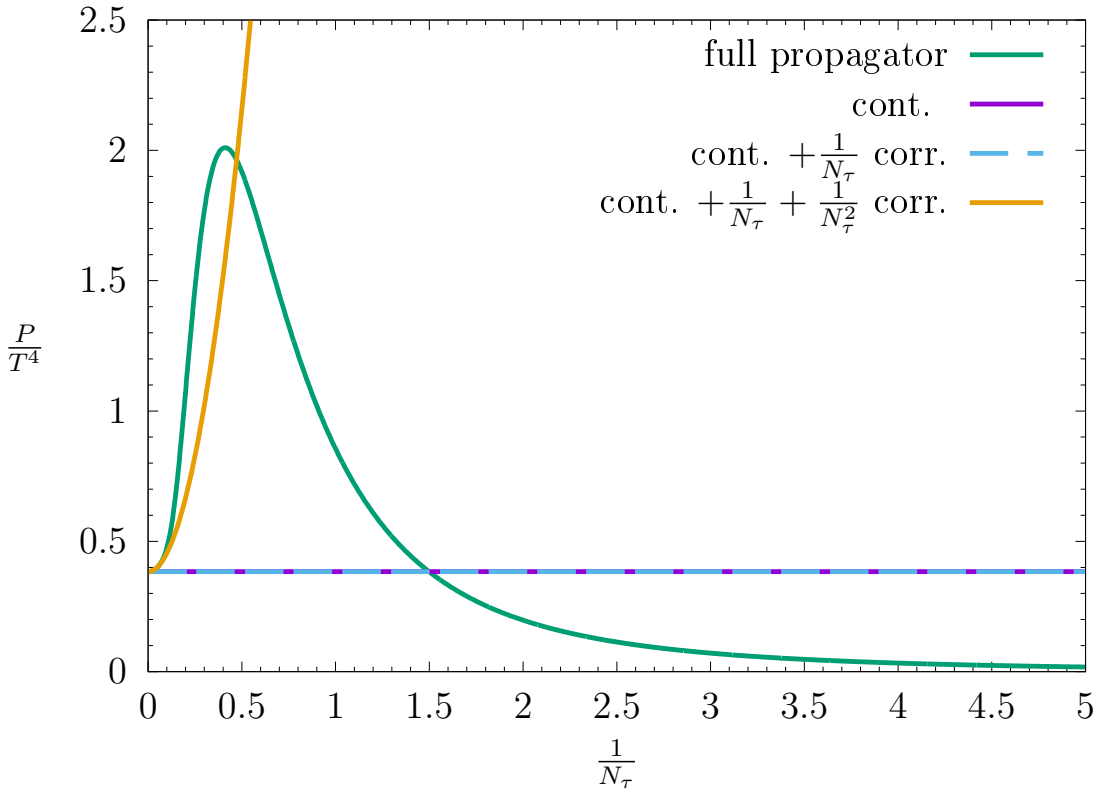

Figure 4.1: The ratio P/T^4 as a function of the inverse finite temporal extent $1/N_\tau$. $m/T = 0$ and $\mu/T = 0$.

The first figure 4.1, is presenting the ratio of P/T^4 as a function of the inverse finite temporal extent $1/N_\tau$ in the case of $m/T = 0$ and $\mu/T = 0$. Since this case corresponds to massless fermions, the first order correction is zero, like it is shown in equation (3.16) and figure 4.2. Thus the light blue line is equal to the purple one. In the case of the second order correction, the expected quadratic behavior is recognizable in figure 4.1, as well as in figure 4.3.

The continuum, here with $\mu/T = 0$, also shows the correct result of $7\pi^2/180 \approx 0.3838$, which has been calculated in equation (3.30).

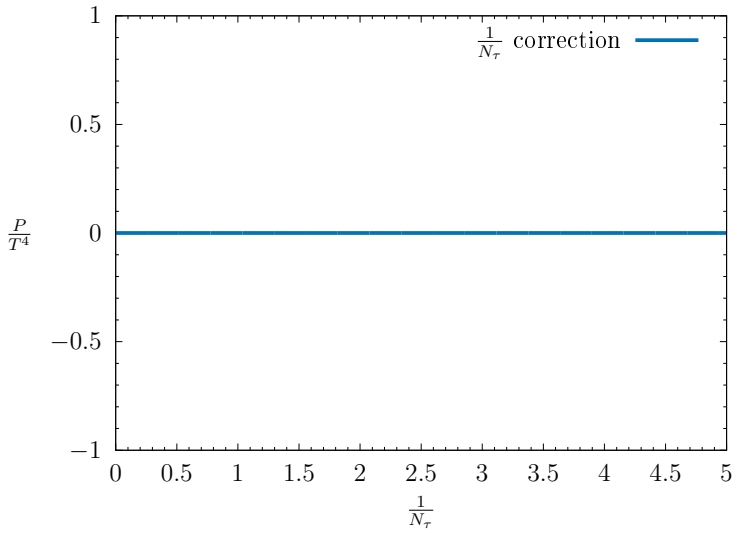

Figure 4.2: The first order correction of the ratio P/T^4 as a function of the inverse finite temporal extent $1/N_\tau$. $m/T = 0$ and $\mu/T = 0$.

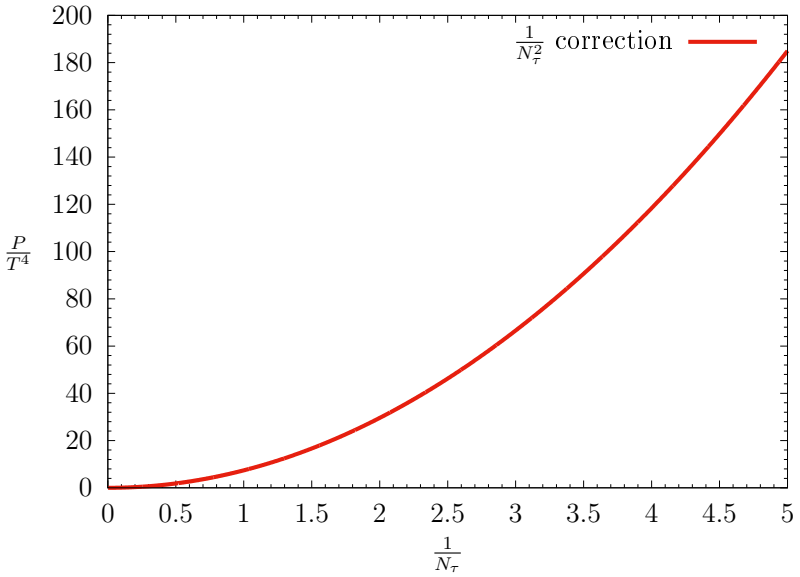

Figure 4.3: The second order correction of the ratio P/T^4 as a function of the inverse finite temporal extent $1/N_\tau$. $m/T = 0$ and $\mu/T = 0$.

4.2 Ratio of P/T^4 for massive fermions

Moving on to the case of massive fermions with $m/T = 0.2$, one can see that the full propagator term has a lower maximum than in the massless case. Similarly, the value of the continuum term is reduced to ≈ 0.3805.

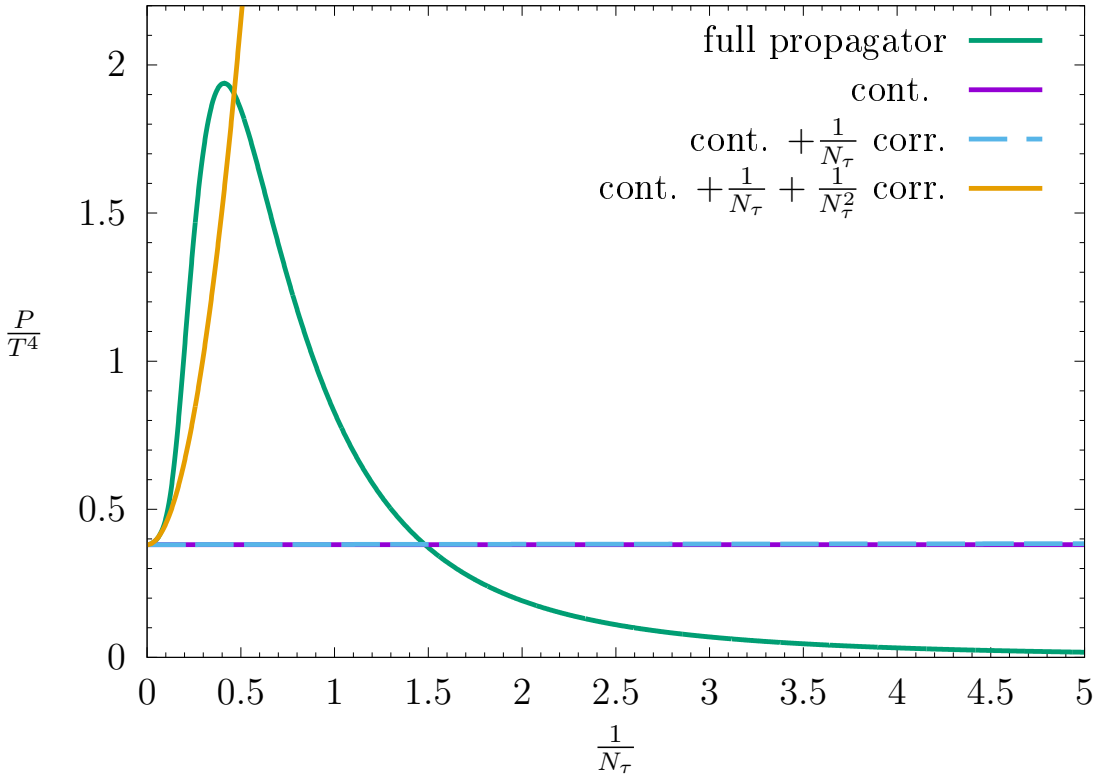

Figure 4.4: The ratio P/T^4 as a function of the inverse finite temporal extent $1/N_\tau$. $m/T = 0.2$ and $\mu/T = 0$.

In the case of massive fermions, the first order corrections now also contribute linearly. However, the first order correction in figure 4.5 is very small. This explains why the differences between the purple and light blue lines in figure 4.4 are not so obvious. Compared to the second order correction in figure 4.6 the first order correction contributes much less.

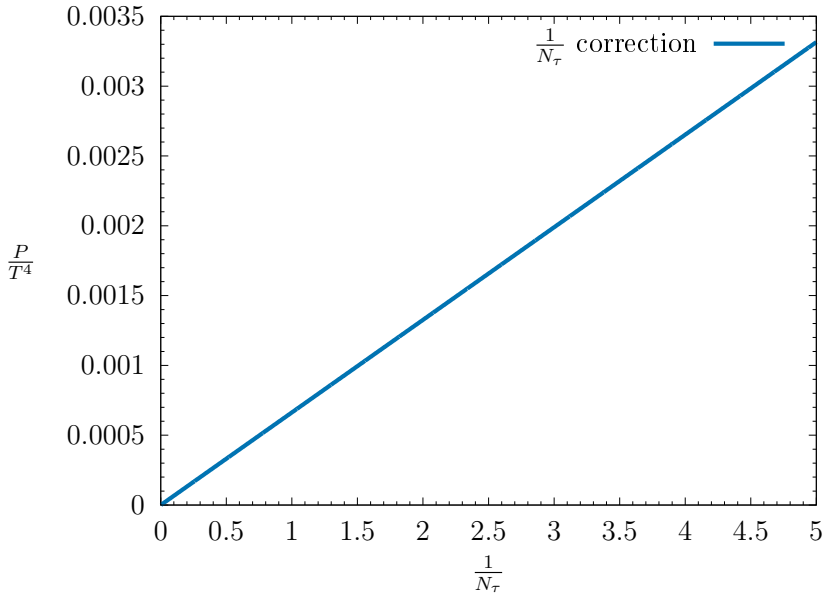

Figure 4.5: The first order correction of the ratio P/T^4 as a function of the inverse finite temporal extent $1/N_\tau$. $m/T = 0.2$ and $\mu/T = 0$.

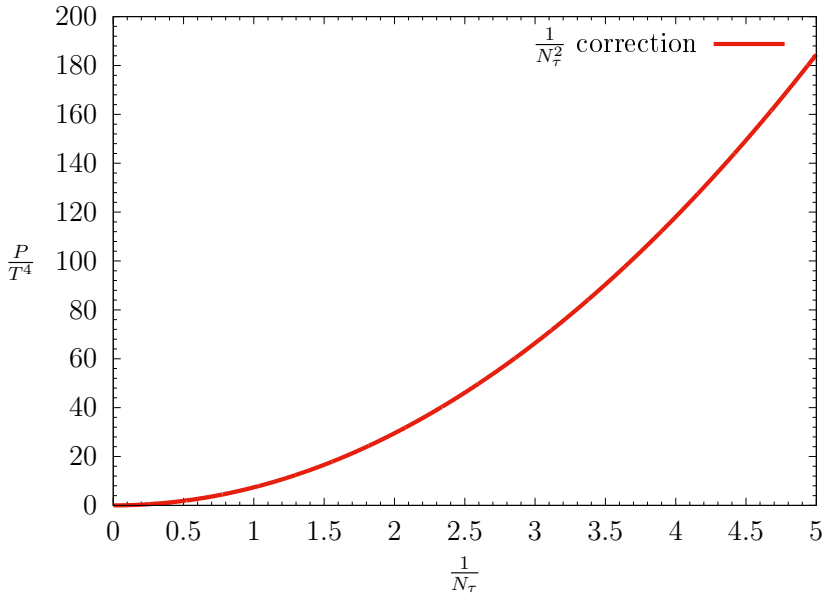

Figure 4.6: The second order correction of the ratio P/T^4 as a function of the inverse finite temporal extent $1/N_\tau$. $m/T = 0.2$ and $\mu/T = 0$.

4.3 Ratio of P/μ^4 for massless fermions

As mentioned above, the ratio between the pressure and the chemical potential, which is described at the end of section 3.3, can be considered, too. Therefore, the ratio of P/μ^4 as a function of the chemical potential $a\mu$ in units of the lattice spacing is illustrated.

Again, the massless case will be considered first; therefore the parameters are chosen as $am = 0$ and $aT = 0.01$. The numerical calculations consist of terms with $1/T$, hence the choice of $aT = 0.01$ is an approximation to the limit of $T \to 0$.

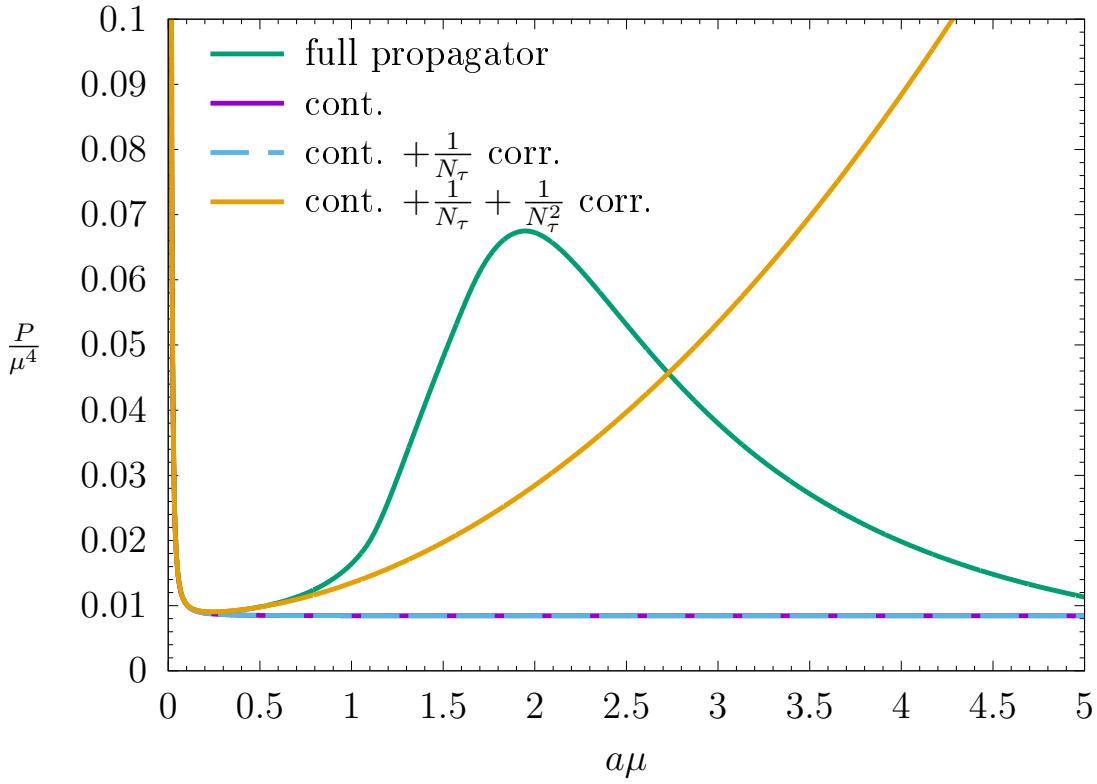

Figure 4.7: The ratio P/μ^4 as a function of the chemical potential $a\mu$. $am = 0$ and $aT = 0.01$.

Following equation (3.30) and using the limit of $T = 0$, the continuum limit corresponds to $15/(180\pi^2) \approx 8.443 \times 10^{-3}$.

The divergent values appearing in the full propagator, as well as in the continuum and the corrections in the interval $a\mu \in [0, 0.25]$, are caused by the dependency of $1/\mu^4$. In the case of a smaller T, this effect will decrease and vanishes in the case of $T = 0$.

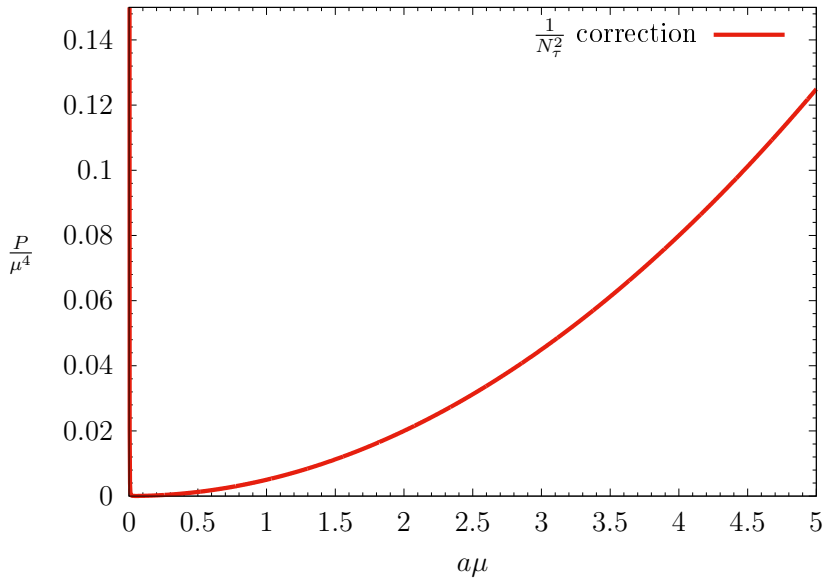

Figure 4.8: The second order correction of the ratio P/μ^4 as a function of the chemical potential $a\mu$. $am = 0$ and $aT = 0.01$.

The first correction also vanishes for the massless case and thus only the second order correction contributes.

4.4 Ratio of P/μ^4 for massive fermions

Comparing the massless case explained above, with the case of massive fermions $m/T = 0.2$, especially the difference in the beginning of the graph becomes obvious. Through the implemented mass the effect of $1/\mu^4$ is suppressed. The full propagator, as well as the continuum part, start at 0 for $a\mu = 0$ and begin to increase as soon as $a\mu > am$ [14, pp. 15–16]. Afterwards the continuum approaches the value $\approx 8.403 \times 10^{-3}$ which is slightly smaller than the value in the massless case.

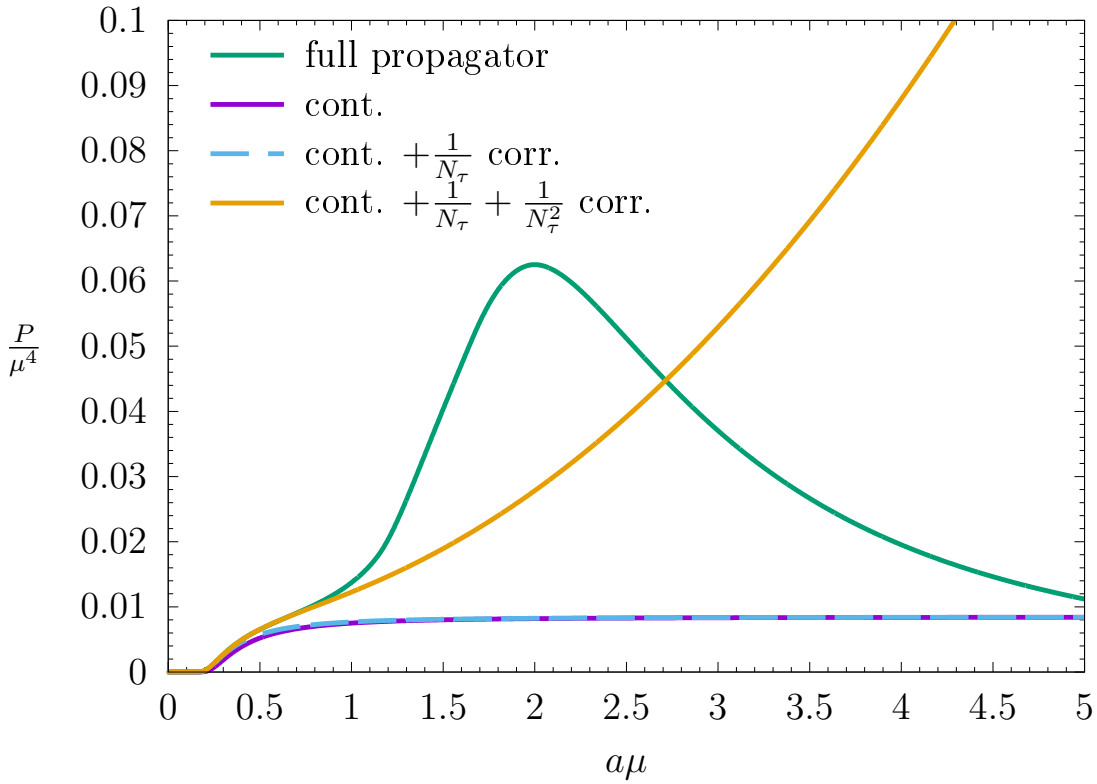

Figure 4.9: The ratio P/μ^4 as a function of the chemical potential $a\mu$. $am = 0.2$ and $aT = 0.01$.

Since the $a\mu$ dependency, instead of the $1/N_\tau$ dependency is considered here, it is noticeable that, the first order correction is no longer linear. It rises very fast to a maximum around $a\mu = 0.3$ before it decreases again.

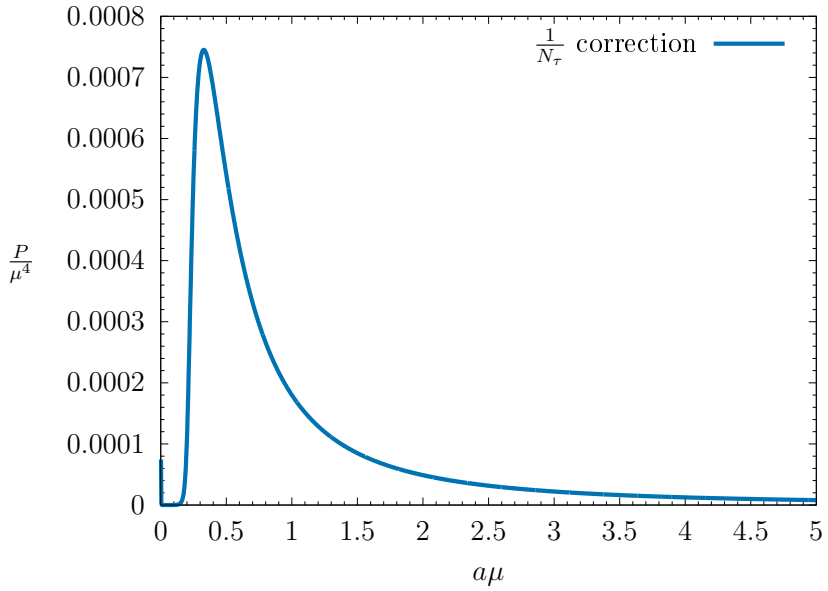

Figure 4.10: The first order correction of the ratio P/μ^4 as a function of the chemical potential $a\mu$. $am = 0.2$ and $aT = 0.01$.

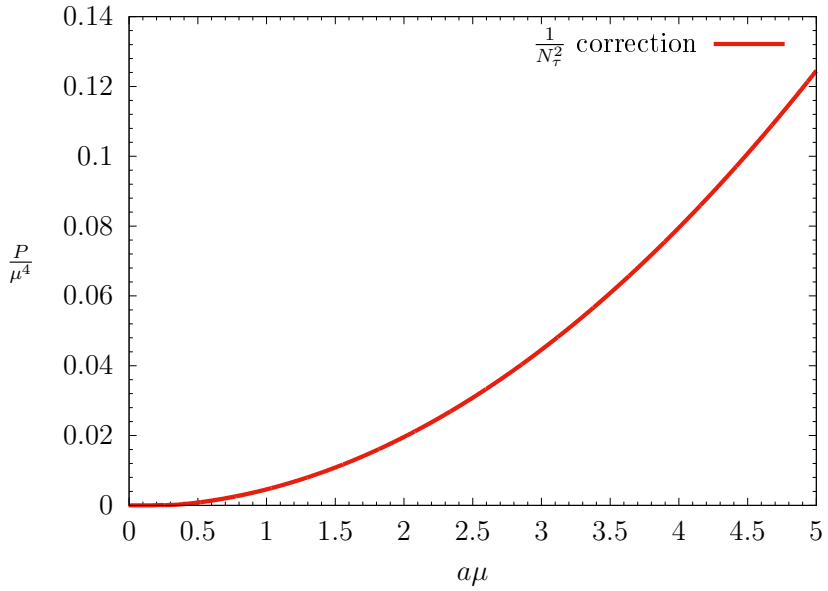

Figure 4.11: The second order correction of the ratio P/μ^4 as a function of the chemical potential $a\mu$. $am = 0.2$ and $aT = 0.01$.

4.5 Ratio of n_B/T^3 for massless fermions

In this section, the ratio of the baryon density and the temperature is considered as a function of the inverse finite temporal extent $1/N_\tau$. Therefore, the fermion density, as it is derived in equations (3.31)–(3.35), is used.

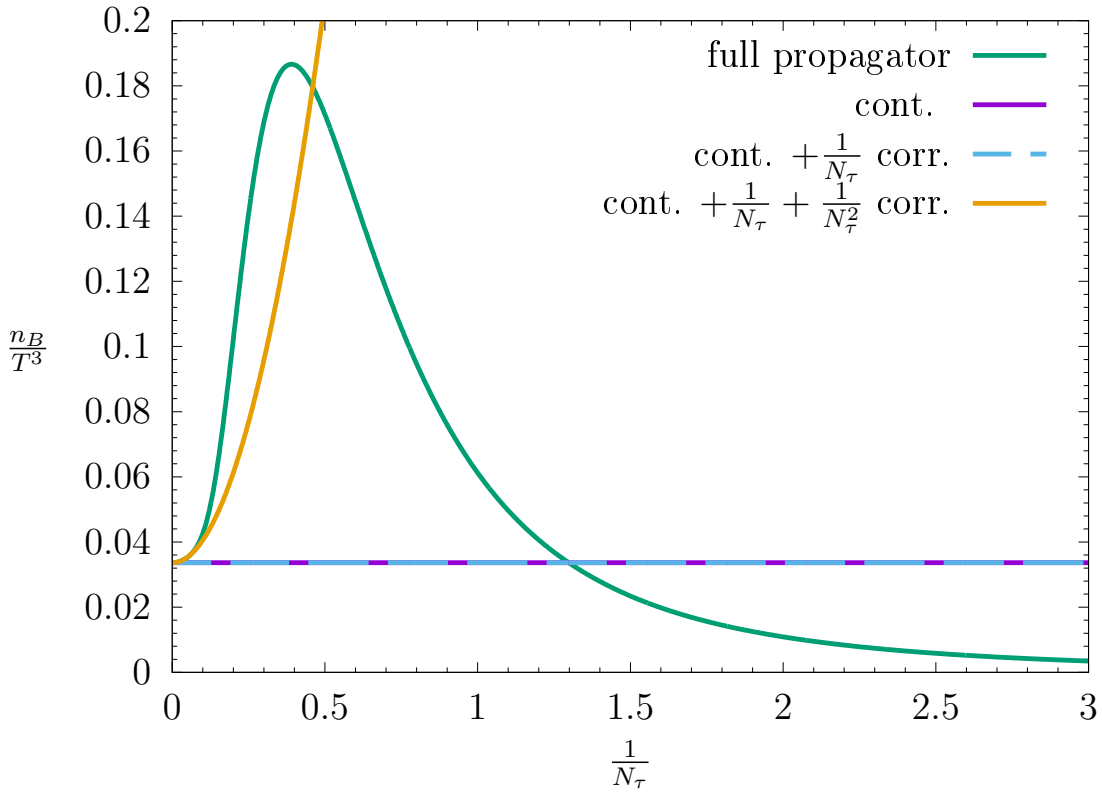

Figure 4.12: The ratio n_B/T^3 as a function of the inverse finite temporal extent $1/N_\tau$. $m/T = 0$ and $\mu/T = 0.3$.

By using the parameters $m/T = 0$ and $\mu/T = 0.3$, the behavior of figure 4.12 is similar to the behavior of figure 4.1. Since the baryon density is a third of the fermion density, the calculated continuum result from equation (3.36) is represented correctly at a value of 0.0336. The full propagator also reaches the correct continuum value for $1/N_\tau \to 0$.

Here, the first order correction is again zero and the second order correction shows the quadratic behavior.

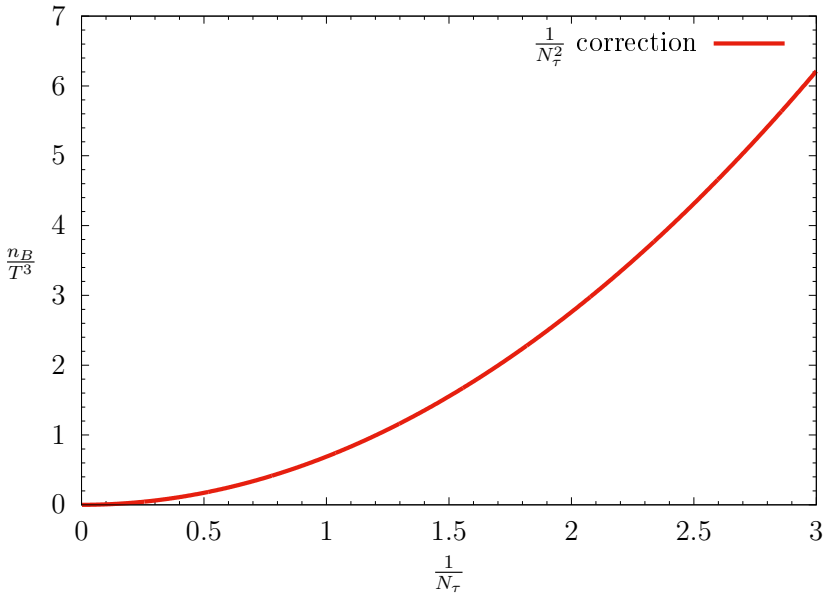

Figure 4.13: The second order correction of the ratio n_B/T^3 as a function of the inverse finite temporal extent $1/N_\tau$. $m/T = 0$ and $\mu/T = 0.3$.

4.6 Ratio of n_B/T^3 for massive fermions

The massive case of the baryon density in relation to the temperature, shows a similar behavior as the massive case of the pressure shown in figure 4.4. Similarly to the case above, the maximum of the full propagator and the value of the continuum are reduced. The continuum part reaches a value of 0.0334.

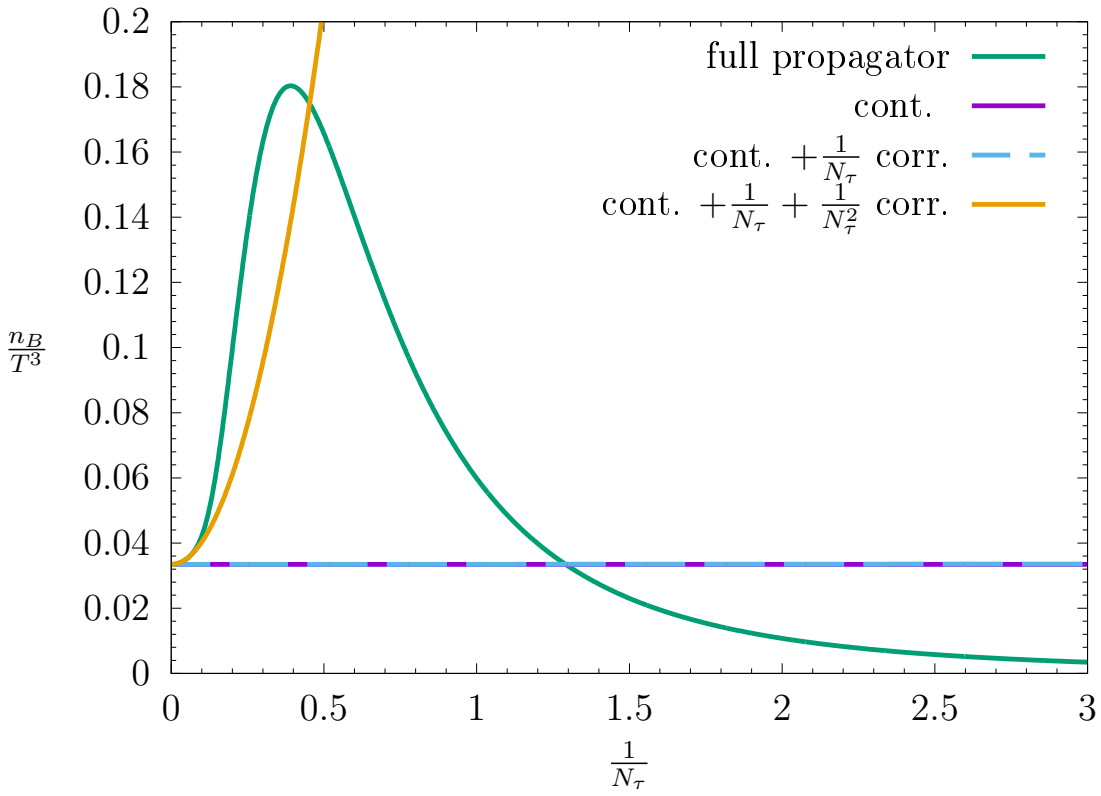

Figure 4.14: The ratio n_B/T^3 as a function of the inverse finite temporal extent $1/N_\tau$. $m/T = 0.2$ and $\mu/T = 0.3$.

Here, the first order correction again contributes linearly to the expanded form; however, the first order correction is once more much smaller than the second order correction.

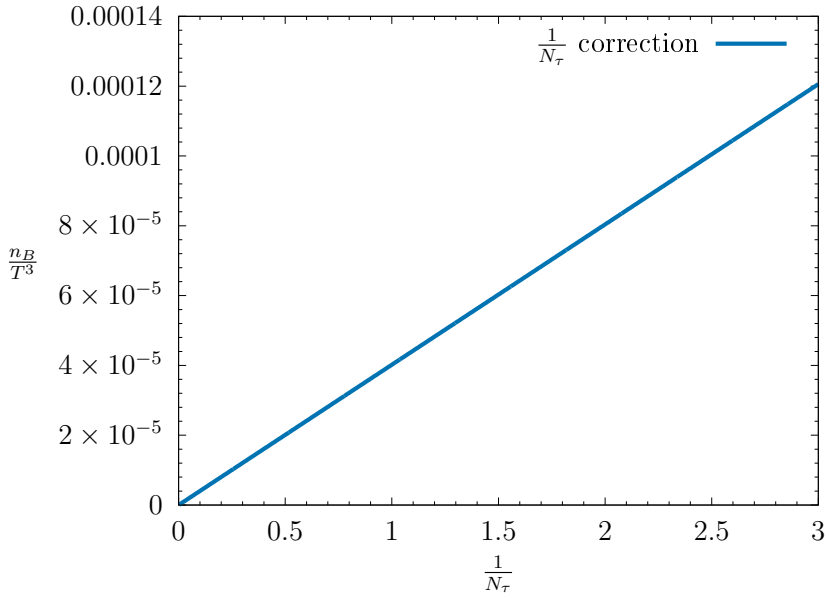

Figure 4.15: The fist order correction of the ratio n_B/T^3 as a function of the inverse finite temporal extent $1/N_\tau$. $m/T = 0.2$ and $\mu/T = 0.3$.

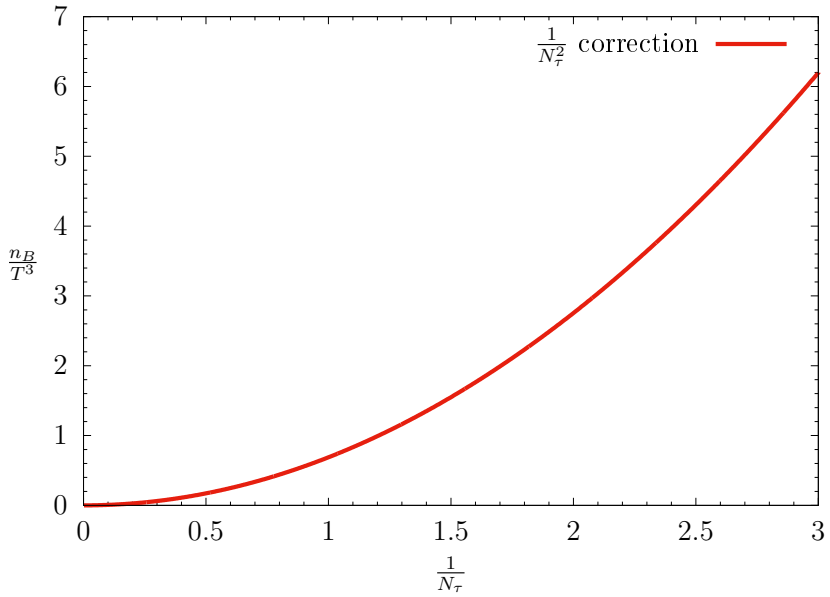

Figure 4.16: The second order correction of the ratio n_B/T^3 as a function of the inverse finite temporal extent $1/N_\tau$. $m/T = 0.2$ and $\mu/T = 0.3$.

4.7 Ratio of n_B/μ^3 for massless fermions

Like the pressure, the baryon density can also be considered in relation to the chemical potential. Hence, the ratio of n_B/μ^3, as a function of $a\mu$ in units of the lattice spacing, is shown in the following.

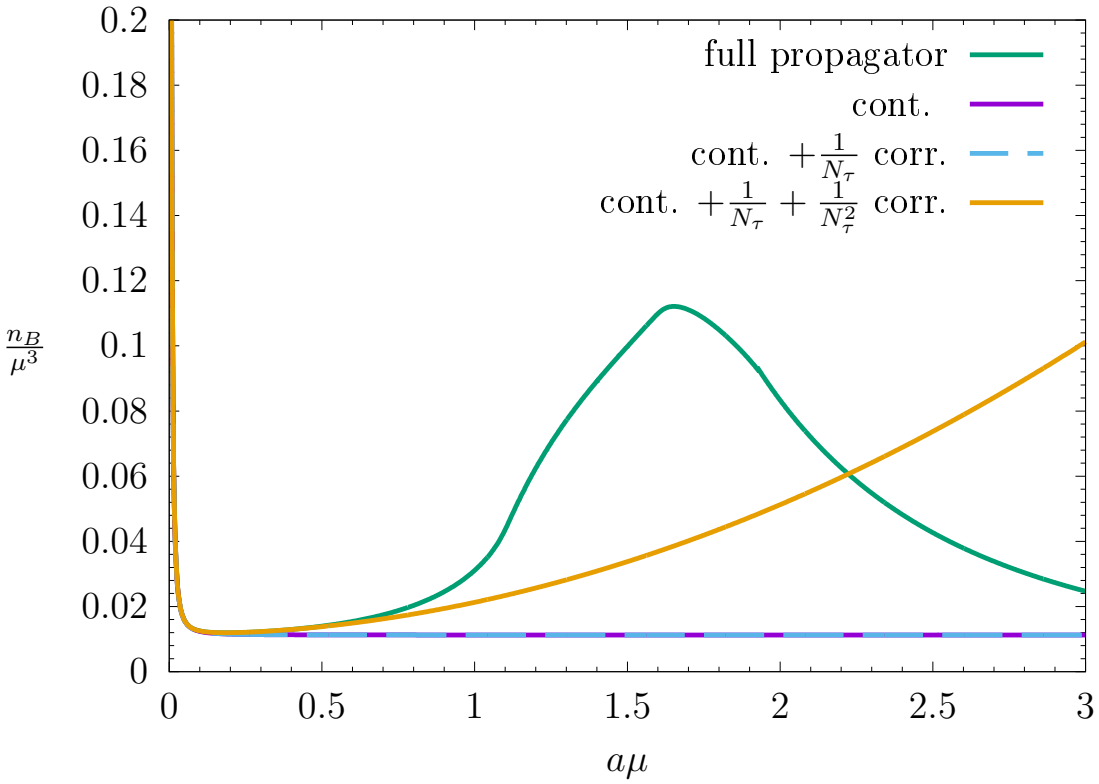

Figure 4.17: The ratio n_B/μ^3 as a function of the chemical potential $a\mu$. $am = 0$ and $aT = 0.01$.

The deviations occurring here in the range of $a\mu \in [0, 0.1]$ are again caused by the dependency of $1/\mu^3$. As in the case of pressure, this behavior decreases when T becomes smaller and vanishes for $T = 0$.

Equation (3.36) and the limit of $T \to 0$ can be used to describe the massless continuum value of n_B/μ^3. The continuum line is representing the right value of $1/(9\pi^2) \approx 1.125 \times 10^{-2}$.

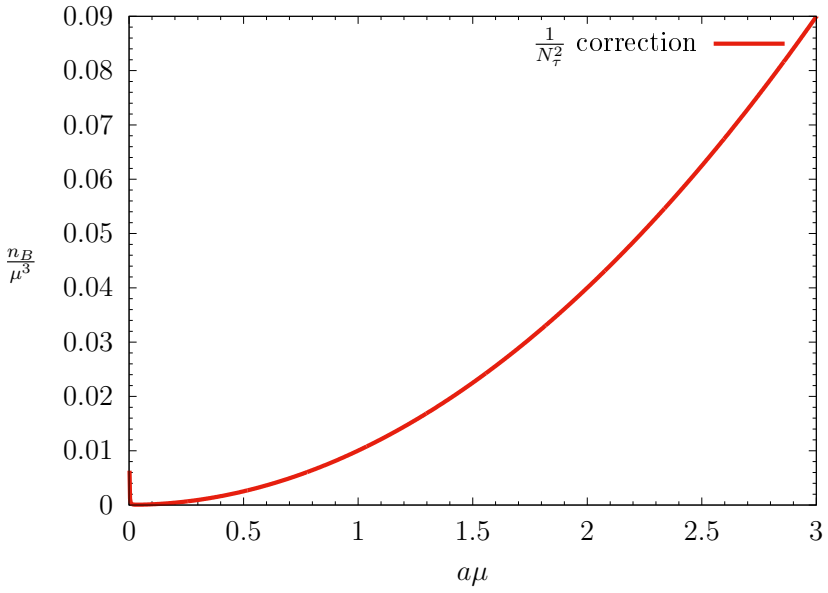

Figure 4.18: The second order correction of the ratio n_B/μ^3 as a function of the chemical potential $a\mu$. $am = 0$ and $aT = 0.01$.

4.8 Ratio of n_B/μ^3 for massive fermions

In the case of massive fermions, with $am = 0.2$, the same effect which has been discussed in section 3.4 and in section 4.4 on pressure, occurs at the beginning of the graph. The full propagator and the continuum curve are zero in the region where $a\mu$ is smaller than am. As soon as $a\mu$ grows larger than am, both curves start to rise. The continuum then approaches a value of 1.123×10^{-2}.

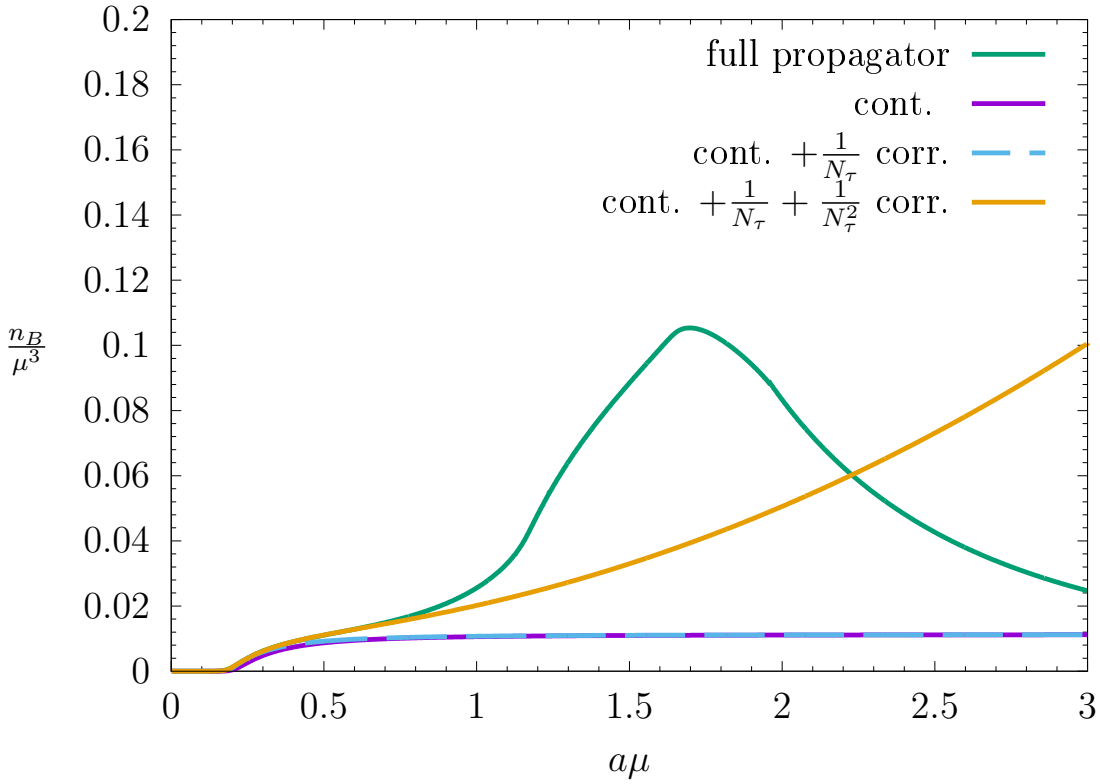

Figure 4.19: The ratio n_B/μ^3 as a function of the chemical potential $a\mu$. $am = 0.2$ and $aT = 0.01$.

The first order correction does not behave linearly as it did in section 4.4. Additionally, the first order correction quickly reaches a maximum around $a\mu = 0.25$ and decreases again.

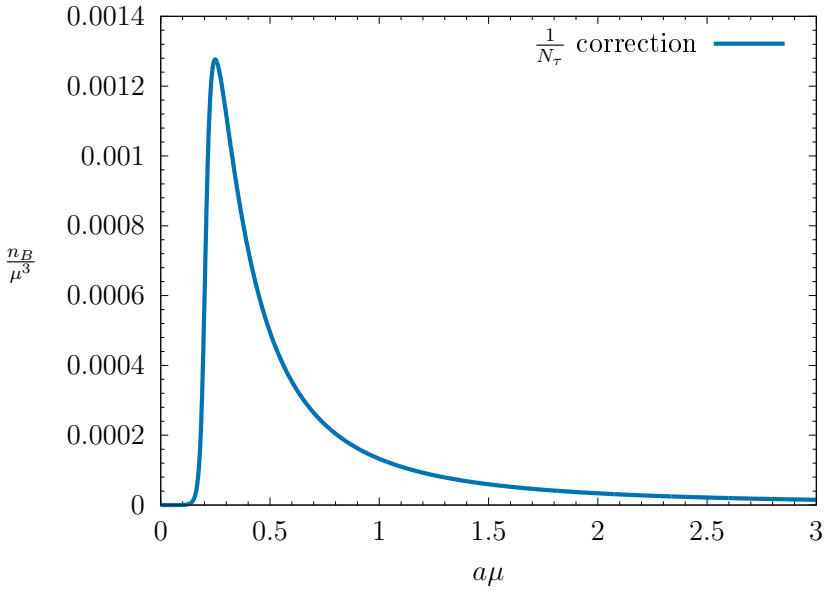

Figure 4.20: The first order correction of the ratio n_B/μ^3 as a function of the chemical potential $a\mu$. $am = 0.2$ and $aT = 0.01$.

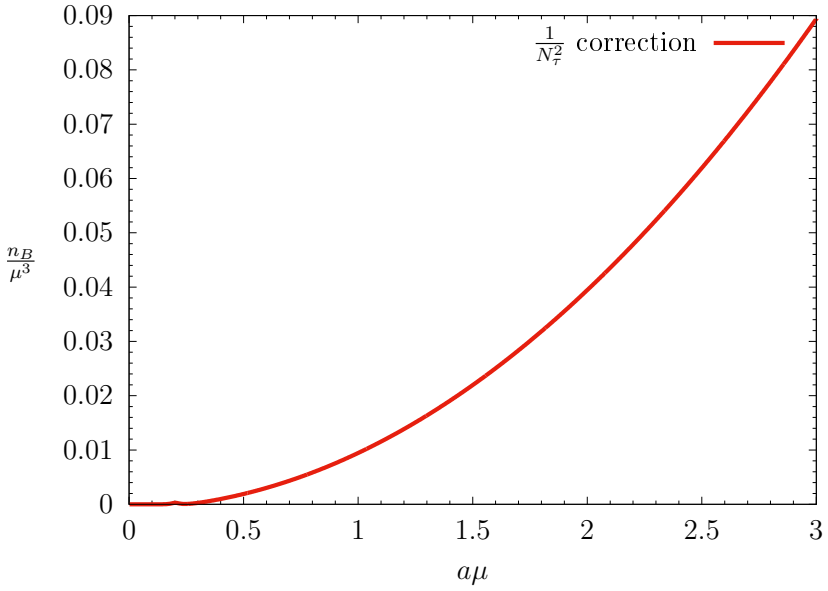

Figure 4.21: The second order correction of the ratio n_B/μ^3 as a function of the chemical potential $a\mu$. $am = 0.2$ and $aT = 0.01$.

5 Summary

In this thesis, lattice cut-off effects of thermodynamic quantities, with chemical potential and massive Wilson fermions, are calculated; therefore an introduction to continuum and lattice QCD, Wilson fermions and thermodynamic quantities is given. Starting from this, the mass is incorporated into the relevant equations, of [5, pp. 1–6], which were used to numerically calculate the cut-off effects.

The results of the calculations, with massless and massive Wilson fermions, were then graphically represented by the unexpanded, as well as the first and second order corrections of the expanded quantities. Through the graphical presentation of the cut-off effects, a few similarities between the massless and massive case were found.

For massless fermions, the corrections to the continuum result are known to start at the second order correction. Once the mass is included into the terms of the cut-off effects, a first order correction is found as well. Furthermore, the included mass causes a suppression of quantities such as the pressure and the density, as long as the chemical potential is smaller than the mass. As soon as the chemical potential becomes larger than the mass, this effect vanishes and the behavior is similar to the massless case.

Thus, the mass dependence of the thermodynamic quantities seems to be relevant especially in those regions, where the chemical potential is smaller than the mass.

List of Figures

Bibliography

[1] Wikipedia. *"Standard model – wikipedia, the free encyclopedia"*. [Online; accessed 26-February-2018]. Feb. 2018. URL: https://en.wikipedia.org/wiki/Standard_Model.

[2] Heinz J Rothe. *Lattice Gauge Theories: An Introduction Third Edition*. Vol. 82. World Scientific Publishing Company, 2012.

[3] Christopher Pinke. "Lattice QCD at finite temperature with Wilson fermions". In: (2014).

[4] Owe Philipsen. "Lattice QCD at non-zero temperature and baryon density". In: (2010).

[5] P Hegde et al. "Lattice cut-off effects and their reduction in studies of QCD thermodynamics at non-zero temperature and chemical potential". In: *The European Physical Journal C-Particles and Fields* 55.3 (2008), pp. 423–437.

[6] Christof Gattringer and Christian B Lang. *Quantum Chromodynamics on the Lattice: An Introductory Presentation, volume 788 of Lecture Notes in Physics*. Springer, Berlin/Heidelberg, 2010.

[7] Wikipedia. *"Lattice QCD – wikipedia, the free encyclopedia"*. [Online; accessed 26-February-2018]. Feb. 2018. URL: https://en.wikipedia.org/wiki/Lattice_QCD.

[8] Gernot Münster. "Lattice quantum field theory". In: *Scholarpedia* 5.12 (2010), p. 8613.

[9] H-Th Elze, K Kajantie, and J Kapusta. "Screening and plasmon in QCD on a finite lattice". In: *Nuclear Physics B* 304 (1988), pp. 832–849.

[10] Ava Khamseh. "Introduction to Lattice QCD: The Basics". In: (2014).

[11] Lars Zeidlewicz. "The thermal transition of quantum chromodynamics with twisted mass fermions". In: (2011).

[12] Stefan B Ruester. "The phase diagram of neutral quark matter". In: *arXiv preprint nucl-th/0612090* (2006).

[13] W Bietenholz and U-J Wiese. "Perfect actions with chemical potential". In: *Physics Letters B* 426.1 (1998), pp. 114–120.

[14] Gert Aarts. *QCD at non zero chemical potential and the sign problem.* [Online; accessed 02-20-2018]. Aug. 2012. URL: `http://www.int.washington.edu/PROGRAMS/12-2c/week2/aarts_01.pdf`.

[15] Numerical Algorithms Group. *NAG Library Routine D01FCF.* [Online; accessed 26-February-2018]. URL: `https://www.nag.co.uk/numeric/fl/nagdoc_fl24/html/D01/d01fcf.html`.

Selbstständigkeitserklärung

Erklärung nach §30 (12) Ordnung für den Bachelor- und dem Masterstudiengang

Hiermit erkläre ich, dass ich die Arbeit selbstständig und ohne Benutzung anderer als der angegebenen Quellen und Hilfsmittel verfasst habe. Alle Stellen der Arbeit, die wörtlich oder sinngemäß aus Veröffentlichungen oder aus anderen fremden Texten entnommen wurden, sind von mir als solche kenntlich gemacht worden. Ferner erkläre ich, dass die Arbeit nicht - auch nicht auszugsweise - für eine andere Prüfung verwendet wurde.

Datum: _____ Unterschrift: _____